to the single aquo ligand for the HEDTA complex. This is in accord with the expectation for an inner-sphere mechanism, which clearly is required for the formation of the Fe–C bond.

(c) The stability constants of the ferric–carbon entities are large, $K_{10} \sim 10^5\ M^{-1}$. Thus, the overall free energy gains for reaction 10 are 6.9 and 7.3 kcal/mol for NTA and HEDTA, respectively. It is interesting to note that the corresponding equilibrium constant for the formation of $(H_2O)NTA\text{-}Fe^{III}CH_3^-$ is lower, $2.5 \times 10^3\ M^{-1}$.[13] This result indicates that the iron–carbon bond in $L\text{-}Fe^{III}CO_2^{2-}$ is stronger than in $L\text{-}Fe^{III}CH_3^-$.

The results obtained for the ferrous HEDTA complex show that the intermediate observed by Rush and Koppenol[6] (upon mixing this complex with H_2O_2 in the presence of formate) is not the suggested $Fe^{II}HEDTA^{\bullet}$ ligand radical (formed from the decomposition of the ternary complex of the ferrous–peroxo complex with formate) but the complex with the metal–carbon σ-bond. This conclusion results from the fact that both the absorption spectrum and their reported kinetics agree well with our observation for the $HEDTA\text{-}Fe^{III}CO_2^{2-}$. The $HEDTA\text{-}Fe^{II}$ possibly reacts with H_2O_2 to yield either the $OH^{\bullet}$ radical or the $HEDTA\text{-}Fe^{II}H_2O_2$ complex, which subsequently reacts with excess concentration of HCO_2^- via reaction 16. The CO_2^- radical

$$OH^{\bullet}/L\text{-}Fe^{II}H_2O_2 + HCO_2^- \rightarrow H_2O/L\text{-}Fe^{III} + CO_2^- \quad (16)$$

produced reacts via reactions 10 and 11. Taking the concentrations used by Rush and Koppenol[6] and the known specific rate constants of the relevant reactions, the calculations show that in their experiments the $HEDTA\text{-}Fe^{III}CO_2^{2-}$ was formed within the mixing time of $HEDTA\text{-}Fe^{II}$ with H_2O_2 in the presence of formate.

It is interesting to note that the decomposition reaction (11) at pH 7, which involves the attack of CO_2^- on the $Fe^{III}CO_2^{2-}$ complex, yields equimolar concentrations of CO_2 and CO in contrast to the bimolecular reaction of CO_2^- in the absence of $L\text{-}Fe^{II}$, which yields oxalate anion. The iron complex thus acts as a catalyst for the disproportionation reaction (eq 17). The

$$L\text{-}Fe^{III}CO_2^{2-} + CO_2^- + 2H^+ \rightarrow L\text{-}Fe^{II} + CO + CO_2 + H_2O \quad (17)$$

data are insufficient for a detailed analysis of the mechanism of this reaction, which is probably a model reaction to processes occurring in the catalytic reduction of CO_2, e.g. in electrocatalytic processes.[19]

It would be very interesting to study the same system with more complicated carbon radicals, e.g. glycerol, ribose, ATP, etc., and to see whether in these systems degradation of the ligand would be the result of the decomposition reaction of the metal–carbon complex. These systems might serve as a model for biological damage, where, through an intermediate with a metal–carbon σ-bond, the damage occurs site specifically.

Acknowledgment. This work was supported in part by grants from the Israel Academy of Sciences and Humanities, the Planning and Granting Committee of the Council of Higher Education and the Israel Atomic Energy Commission, and the Council of Tobacco Research. D.M. thanks Irene Evens for her continued interest and support.

Registry No. NTA, 139-13-9; HEDTA, 150-39-0; $(H_2O)(NTA)\text{-}Fe^{III}CO_2^{2-}$, 114198-67-3; $(HEDTA)Fe^{III}CO_2^{2-}$, 114198-68-4; N_2O, 10024-97-2; $Co(NH_3)_6^{3+}$, 14695-95-5; sodium formate, 141-53-7; ferrous sulfate, 7720-78-7; ferrous ammonium sulfate, 10045-89-3; ferric ammonium sulfate, 7783-83-7.

(19) Beley, M.; Collin, J. P.; Rupert, R.; Sauvage, J. P. *J. Am. Chem. Soc.* **1986**, *108*, 7461.

Anisotropic Exchange in the $Co_2(EDTA)\cdot 6H_2O$ and $CoCu(EDTA)\cdot 6H_2O$ Bimetallic Ordered Chains. Low-Temperature Investigation of the Thermal and Magnetic Properties

E. Coronado,[†,§,1] M. Drillon,*[,†] P. R. Nugteren,[‡] L. J. de Jongh,[‡] and D. Beltran[§]

Contribution from the Département Science des Matériaux-EHICS, 1, rue B. Pascal 67008, Strasbourg, France, Kamerlingh Onnes Laboratorium, Leiden University, P.O. Box 9506, 2300 Ra Leiden, The Netherlands, Departamento de Quimica Inorganica, Burjasot, Valencia, Spain. *Received August 28, 1987*

Abstract: We report on the thermal and magnetic behaviors of the chain complexes $Co_2(EDTA)\cdot 6H_2O$ and $CoCu(EDTA)\cdot 6H_2O$ characterized by two different sites for the metal ions. These are octahedrally coordinated either to EDTA ligands or to oxygen atoms of carboxylate groups and four water molecules in order to form alternating zigzag chains. The thermodynamic properties (EPR, high field magnetization, specific heat, and magnetic susceptibility) are discussed in terms of an Ising chain model with regularly or alternatingly spaced sites. It is emphasized, for the first time, that the different g values at different (alternating) sites give rise to a ferrimagnetic-like behavior even for a large dimerization of the chains.

Recently, much experimental and theoretical effort has been devoted to the properties of ordered bimetallic systems, in particular to what is currently referred to as 1d ferrimagnets.[2-9] These may be defined as two sublattice chains in which one sublattice does not compensate the other, due to different spins or also to different coordination environments for the metal ions on each sublattice. Several physical situations, related to real systems, have been considered and solved rigorously. Thus, closed-form expressions of the thermodynamic quantities of interest

[†] Département Science des Materiaux-EHICS.
[‡] Kamerlingh Onnes Laboratorium.
[§] Departamento de Quimica Inorganica.

(1) Permanent address: Departamento de Quimica Inorganica, Valencia, Spain.
(2) Drillon, M.; Coronado, E.; Beltran, D.; Curely, J.; Georges, R.; Nugteren, P. R.; de Jongh, L. J.; Genicon, J. L. *J. Magn. Magn. Mater.* **1986**, *54-57*, 1507.
(3) Drillon, M.; Coronado, E.; Beltran, D.; Georges, R. *J. Appl. Phys.* **1985**, *57*, 3353.
(4) Coronado, E.; Drillon, M.; Fuertes, A.; Beltran, D.; Mosset, A.; Galy, J. *J. Am. Chem. Soc.* **1986**, *108*, 900 and references therein.

0002-7863/88/1510-3907$01.50/0

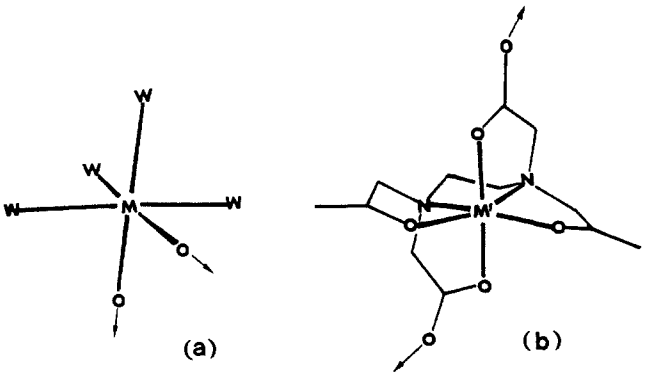

Figure 1. View of the "hydrated" and "chelated" metal environments in the MM'(EDTA)·6H_2O complexes.

were derived when the interactions between nearest neighbors along the chain are of the Ising type, with (quantum–quantum) or (quantum–classical) spin sublattices.[5,6] In the limit of isotropic exchange coupling (Heisenberg model), the problem was shown to be soluble in the classical limit,[7] $S = \infty$, while the solutions for the quantum chain were obtained by numerical computations; the limiting behavior of the infinite chain was simply determined from the exact solutions for finite closed chains $(S_a–S_b)_N$, extrapolated to the thermodynamic limit $(N \rightarrow \infty)$.[3,8]

All these ferrimagnetic chain systems have in common characteristic variation of the curves of $X \cdot T = f(kT/J)$, namely a minimum at an intermediate value of kT/J, and a divergence at lower temperature, according to the power law T^{-a} ($a = 0.8–1$).

Several examples of structurally ordered bimetallic chains have been reported so far.[4,9] Among these, the series MM'(EDTA)·6H_2O (M and M' refer to divalent transition metals) offers a large diversity of chain systems showing a ferrimagnetic-like behavior.[2-4] The aim of this paper is to show that very similar magnetic features are obtained in chain complexes characterized by alternating Landé factors, only.

We will discuss here the thermal and magnetic properties of two complexes of the above series, Co_2(EDTA)·6H_2O and CoCu(EDTA)·6H_2O, abbreviated hereafter as [CoCo] and [CoCu]. Their structure has been reported elsewhere[4] and consists of infinite zigzag chains, built up from two alternating octahedral sites denoted as "hydrated" and "chelated", according to the local environments (Figure 1). The metal M is coordinated to four water molecules and two oxygen atoms of bridging carboxylate groups, while M' is hexacoordinated to the EDTA ligand. Thus, in [CoCu] the cobalt(II) ion occupies the "hydrated" site, whereas the copper(II) is located in the "chelated" one.

Futhermore, the M–M' distances along the chain are slightly alternating, as a consequence of different bridging carboxylate topologies. For example, in [CoCo] the two consecutive Co–Co distances are 5.581 and 5.994 Å, and the associated bridging carboxylate angles are equal to 123.4° and 124.8°, respectively. Accordingly, the chain may be schematized as

$$\ldots M(H_2O)_4O_2 \text{---} M'(EDTA) \ldots M(H_2O)_4O_2 \text{---} M'(EDTA)$$

where dotted and full lines refer to the two different exchange pathways.

From the magnetic point of view, this implies that there should be an alternation not only in the size of the magnetic moment but also in the exchange coupling, as indicated in the following sketch

$$\ldots S(g_a) \text{---} S'(g_b) \ldots S(g_a) \text{---} S'(g_b) \ldots$$

Here S (S') and g_a (g_b) are the spin values and the Landé factors at each site.

In a preliminary study,[10] we have reported the magnetic behavior of [CoCo] in the temperaure range 2–100 K. The variation of the magnetic susceptibility below 20 K was shown to agree with that of an antiferromagnetic exchange-coupled $S = 1/2$ chain. Accordingly, we have proposed an analysis of the magnetic data on the basis of Heisenberg and Ising models, by assuming identical g values on both sites. In fact, due to the weakness of the exchange coupling, further investigation at lower temperature was required to draw more definite conclusions about the validity of the proposed models.

In this paper, we investigate the thermal and magnetic properties of the [CoCo] and [CoCu] complexes in the very low-temperature region. These properties are discussed on the basis of the Ising chain model by assuming alternating Landé factors and also an alternation of the interaction between nearest neighbors. For the first time, the ferrimagnetic character is reported experimentally in spin-1/2 systems and correlated to sublattices with different g factors.

Experimental Section

EPR measurements were recorded on a Bruker ER 200D X-band spectrometer.

Susceptibility measurements were performed in the temperature range 0.15–4.2 K with two different techniques. The low-temperature data were taken in an adiabatic demagnetization apparatus by means of a mutual inductance bridge operating at 35 Hz. The susceptibility data, obtained in arbitrary units, were first corrected for the signal of the empty coil system and then scaled in the range 0.15–2.1 K on the results obtained in a differential susceptibility setup operating at 82.8 Hz in the temperature range 1.3–4.2 K. The data, corrected for the diamagnetism of the constituent atoms, are given with an accuracy better than 10^{-5} emu·mol^{-1} for the susceptibilities, and a temperature uncertainty of 0.01 K. On the other hand, high field magnetization measurements were carried out at 1.1 K, in the range 0–20 T, with a pulsed field apparatus.

Specific heat measurements were performed in the temperature range 0.07–30 K. Conventional heat-pulse techniques have been used. The low-temperature specific heat data (0.07–1.5 K) were taken in an adiabatic demagnetization apparatus with magnetic thermometry. The powdered samples were mixed with Apiezon-N grease for thermal contact. A pumped ^{4}He apparatus equipped with a mechanical heat switch was used for the high-temperature measurements (1.4–30 K), with germanium thermometry. A small amount of ^{3}He gas was used to ensure thermal contact between the sample and the calorimeter.

Description of the Results

EPR Spectra. The compounds reported here involve metal ions in very different surroundings. The g components of Cu(II) occupying the chelated site can be estimated from EPR spectra recorded on a Cu-doped [ZnZn] sample. At room temperature, one obtains an axial spectrum ($g_\parallel = 2.27$ and $g_\perp = 2.02$) with the parallel component of the hyperfine coupling equal to 159 G.

The g values of Co(II) at the two sites were roughly estimated from powder EPR measurements carried out at 4 K on [MgCo] and [CoNi] samples.[10] In fact, the estimates can be improved from measurements on Co-doped [ZnZn] samples. Due to the random occupation of both sites by cobalt ions,[11] the spectra contain the features of both environments (Figure 2). On the basis of findings reported for [MgCo], it is possible to associate the signals centered around 10.1, 1.43, and 1.24 to g components of the "chelated" cobalt ion. In turn, the central part of the spectrum may be attributed to the "hydrated" cobalt. This last ion shows an axial spectrum ($g_\parallel = 5.905$, $g_\perp = 3.88$) and an eight-line hyperfine structure on each g component ($A_\parallel = 7.5$ G, $A_\perp = 6.4$ G), in agreement with the nuclear spin of cobalt. Such features agree well with those found for this ion in related "hydrated" environments.[12]

(5) Georges, R.; Curely, J.; Drillon, M. *J. Appl. Phys.* **1985**, *58*, 914.
(6) Curely, J.; Georges, R.; Drillon, M. *Phys. Rev. B.* **1986**, *33*, 6243.
(7) Drillon, M.; Coronado, E.; Beltran, D.; Georges, R. *Chem. Phys.* **1983**, *96A*, 413.
(8) Drillon, M.; Gianduzzo, J. C.; Georges, R. *Phys. Lett.* **1983**, *96A*, 413.
(9) Gleizes, A.; Verdaguer, M. *J. Am. Chem. Soc.* **1984**, *106*, 3727. Verdaguer, M.; Julve, M.; Michalowicz, A.; Kahn, O. *Inorg. Chem.* **1983**, *22*, 2624.
(10) Coronado, E.; Drillon, M.; Beltran, D.; Bernier, J. C. *Inorg. Chem.* **1984**, *23*, 4000.
(11) Escriva, E.; Fuertes, A.; Beltran, D. *Trans. Met. Chem.* **1984**, *9*, 184.
(12) Abragam, A.; Bleaney, B. *Electron Paramagnetic Resonance of Transition Ions*; Clarendon Press: Oxford, 1970.

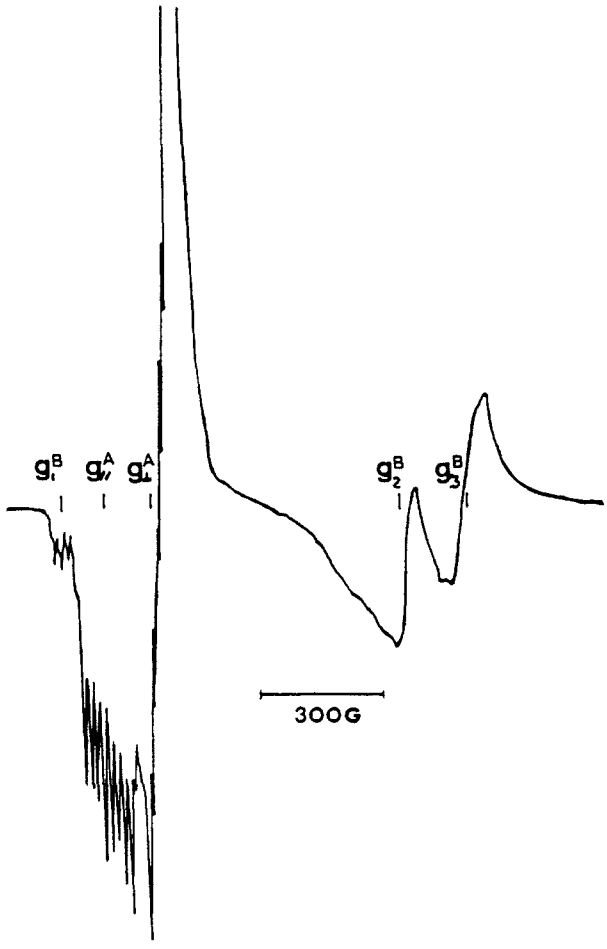

Figure 2. EPR spectrum of Co-doped [ZnZn] sample at 4.2 K.

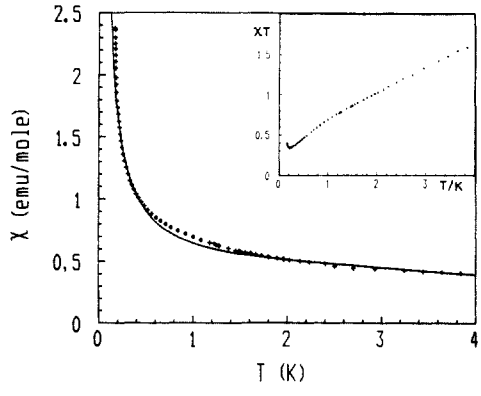

Figure 3. Experimental and theoretical (full line) variation of the magnetic susceptibility of [CoCo] for $J = -10.2$ K, $j = -0.12$ K, $g_a = 3.99$, $g_b = 1.33$, and $g_\perp = 3.03$. The temperature dependence of χT is given in the inset.

Notice that, due to the combined effect of spin-orbit coupling and local distortion of the octahedral sites, it is appropriate to describe high-spin Co(II), at low temperatures, by a Kramers doublet with effective $S = 1/2$ spin.[13] Since copper(II) is also described by a low-lying spin doublet, we assume in the following that at low enough temperature, both [CoCo] en [CoCu] compounds may be viewed as chains of spins $S = 1/2$.

Magnetic Data. The temperature dependence of the zero-field susceptibilities of both [CoCo] and [CoCu] compounds are plotted in Figures 3 and 4, in the range 0.15–4 K. The susceptibility of the [CoCo] compound increases continuously upon cooling down (Figure 3). In fact, it appears in the inset of Figure 3 that the plot of χT versus T is much more revealing to describe such a

(13) Lines, M. E. *J. Chem. Phys.* **1971**, *35*, 2977.

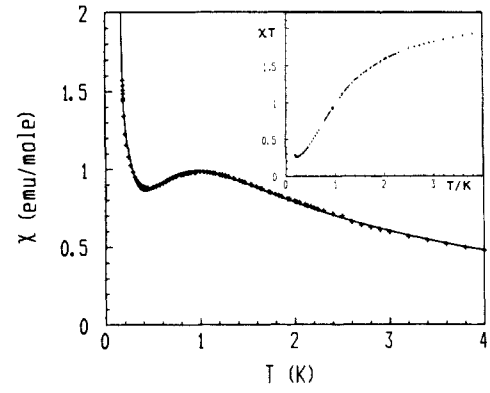

Figure 4. Experimental and theoretical (full line) variation of the magnetic susceptibility of [CoCu] for $J = -3.2$ K, $j = -0.05$ K, $g_a = 4.31$, $g_b = 2.63$, and $g_\perp = 0$. The temperature dependence of χT is displayed in the inset.

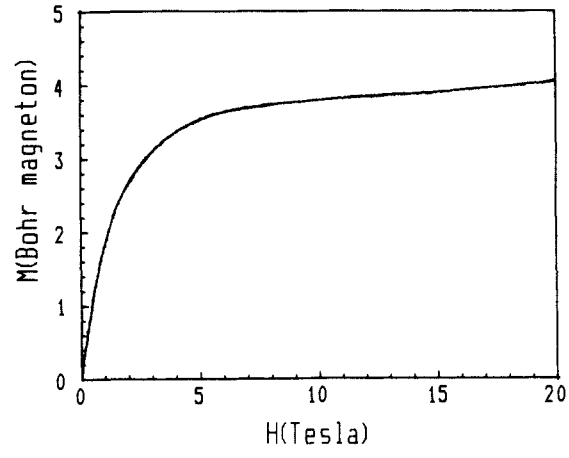

Figure 5. Variation of the magnetization of [CoCu] in pulsed field up to 20 T.

system. When the temperature is lowered, χT decreases, presents a minimum around 0.2 K, and subsequently increases. Such a variation was previously shown to be the signature of 1d ferrimagnets involving either alternating spins or alternating Landé factors.

A similar variation of χT is observed for [CoCu], with a minimum located at the same temperature (Figure 4). Nevertheless, it may be noticed that the $\chi = f(T)$ plot differs significantly, since it exhibits now a rounded maximum around 1 K and a divergence at lower temperatures. In view of the nature of the magnetic sublattices involved in both systems, such a behavior is rather surprising. Thus, in [CoCo] the two local magnetic moments, defined as $g_i S_i$ ($i = a$ or b and $S_i = 1/2$), are nearly equal so that a quasi-antiferromagnetic chain behavior should be observed (a maximum might be expected around 2 K).[10] Contrastingly, the magnetic moments are significantly different in [CoCu] ($g_a/g_b = 2$) so that the occurrence of a susceptibility maximum is quite unexpected. In fact, the above discussion is based on the interaction between isotropic moments, while the EPR findings give evidence of the anisotropic nature of cobalt(II) ion.

The obtained magnetization curve at 1.1 K is shown for the [CoCu] sample in Figure 5. A similar variation is found for the pure cobalt compound. Saturation is reached for an applied field of about 7 T (10 T in the case of [CoCo]) corresponding to 3.7 μ_B (around 4.7 μ_B for [CoCo]). Note that the curve seems to start tangentially to the magnetization axis, which is not observed for the [CoCo] analogue. At low field, a small plateau of height $(g_a - g_b)/2$ should show up, but the temperature is in fact too high to observe it.

Specific Heat Data. The specific heat data of the title compounds are plotted, in the temperature range 70 mK–30 K, in Figures 6 and 7. We note, for both systems, a small minimum

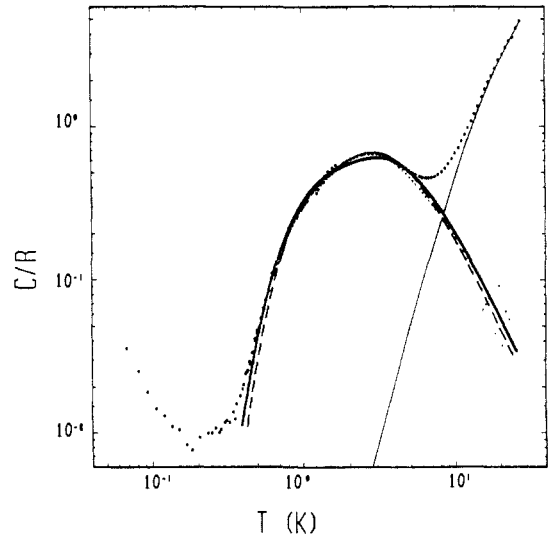

Figure 6. Specific heat data of [CoCo] plotted on log-log scales. Note the asymmetric Schottky-type anomaly around 3 K related to the low-dimensional character of the system. Full and dashed lines refer to the best fits from the J alternating Ising chain and the anisotropic dimer models, respectively.

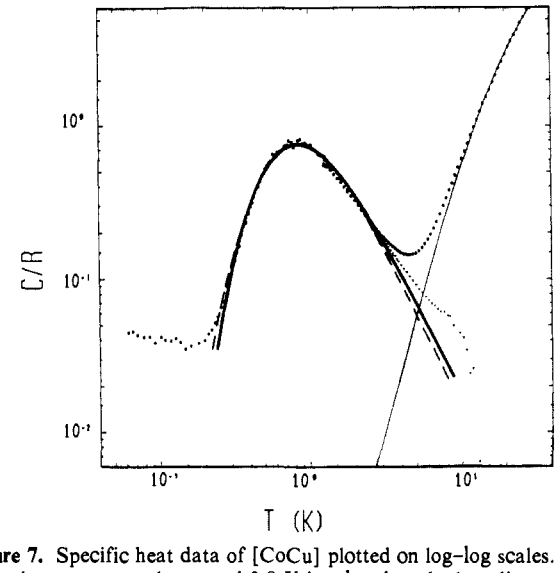

Figure 7. Specific heat data of [CoCu] plotted on log-log scales. The Schottky-type anomaly around 0.8 K is related to the low-dimensional character of the system. Full and dashed lines refer to the best fits from the J alternating Ising chain and the anisotropic dimer model, respectively.

around 0.2 K, then a broad maximum in the data at about 3 K for [CoCo] and 0.8 K for [CoCu], and finally a sharp increase at higher temperatures. No evidence for a λ-type anomaly characteristic of 3d ordering is found down to 70 mK.

From these results, an unambiguous assignment of the various contributions to the specific heat can be made. The lattice contribution, corresponding to the high temperature part of the data, is generally well-approximated by a T^3 law for $T < 10$ K. In fact, in the present series, it is more accurately estimated making use of the specific heat of the isomorphous nonmagnetic compound $Zn_2(EDTA)\cdot 6H_2O$, determined in another experiment. Where necessary, the specific heat of the Zn compound was fitted to the high-temperature data of the magnetic compounds by scaling the temperature axes. On the other hand, an additional contribution arising from nuclear hyperfine interactions appears at very low temperatures, giving rise to a T^{-2} tail. These two contributions are to be subtracted from the raw data in order to obtain the specific heat of magnetic origin. The resulting plots (shown in Figures 6 and 7) are seen to feature Schottky-type anomalies to be attributed, according to magnetic findings, to the 1d character of studied systems.[14] Note that, due to the increasing contribution to the total heat capacity of both the lattice and the addenda with temperature, the accuracy of the magnetic specific heat is decreasing for $T > 10$ K.

The entropy content of the observed magnetic contribution has been determined to be $S/R = 1.34$ for [CoCo] and $S/R = 1.22$ for [CoCu]. Both these values have to be compared with the expected value $S/R = 2\ln 2 = 1.39$, corresponding to two Kramers doublets. This means that the entropy of the [CoCo] compound is 3.5% too small, which is reasonably good. Accordingly, we may consider that the cobalt(II) ion is quite well described by an effective spin 1/2 in the temperature range of the experiment. The entropy of [CoCu] is, on the other hand, 12% too low, which cannot be due to experimental errors, only. It might be caused by an error in the molecular weight (one water molecule is weakly tied) or to uncertainty in the estimate of the lattice contribution deduced from the zinc analogue. Therefore, we decided to increase all the specific heat data by the same scaling factor, in order to obtain the right entropy, before any subsequent analysis.

Theoretical Study of the Two-Sublattice Ising Chain

As a consequence of the strong anisotropy in the g components for Co(II), a large anisotropy of the exchange interaction is expected in the [CoCo] and [CoCu] complexes. An estimate of the amount of anisotropy is given by $J_\parallel/J_\perp = (g_{a\parallel}g_{b\parallel}/g_{a\perp}g_{b\perp})$[15] so that it is mainly fixed by the most distorted ion. Then, the anisotropic Ising model for which exact solutions may, to a large extent, be derived should be closely approximated.

In view of the structural features of both systems, consider a spin-1/2 chain with alternatingly spaced sites, namely with two nearest neighbor interactions ($J - j$), and alternating Landé factors ($g_a - g_b$). The full Hamiltonian is written as

$$\mathcal{H} = -J\sum S^z_{2i-1}S^z_{2i} - j\sum S^z_{2i}S^z_{2i+1} - (g_a\sum S^z_{2i-1} + g_b\sum S^z_{2i})\mu_B H \quad (1)$$

where S^z_i stands for the z component of the spin operator located on site i, μ_B is the Bohr magneton, and H is the external magnetic field.

The problem can be solved exactly by the transfer matrix method if the external field is assumed to be along the quantization axis.[16] Consider the semi-infinite chain ending at site n, and let Z_n be the corresponding partition function. It is readily shown that Z_{n+1}, obtained by adding one extra spin at position $n + 1$, is related to Z_n by a linear transformation. In the specific case of an alternating chain, the parity of the extra spin must be specified, so that for any p index we can write

$$Z_{2p+1} = (T_1)Z_{2p} \text{ and } Z_{2p+2} = (T_2)Z_{2p+1}$$

Then the transfer operator for the chain under consideration is simply given by $(T) = (T_2) \times (T_1)$ which reduces to the following 2 × 2 matrix

$(abs + a^{-1}b^{-1}s^{-1})r$	$(ab^{-1}s + a^{-1}bs^{-1})r$
$(a^{-1}bs + ab^{-1}s^{-1})r^{-1}$	$(a^{-1}b^{-1}s + abs^{-1})r^{-1}$

where

$$a = \exp(J/4kT) \qquad b = \exp(j/4kT)$$
$$r = \exp(g_a u_B H/2kT) \qquad s = \exp(g_b u_B H/2kT)$$

In the limit of very long chains, we show that the effective partition function per pair of sites is nothing but the largest eigenvalue of (T). Analytical expressions for the partition function and the related thermodynamic properties (specific heat, magnetization, magnetic susceptibility) are then easily derived.

(14) See: *Physics in One Dimension*; Bernasconi, J., Schneider, T., Eds.; Springer-Verlag: Berlin, Heidelberg, 1981.
(15) See: de Jongh, L. J. In *Magneto-Structural Correlations in Exchange-Coupled Systems*; Gatteschi, D., Kahn, O., Willett, R. D., Eds.; NATO Advanced Studies Institute, Reidel: Dordrecht, 1984.
(16) Kramers, H. A.; Wannier, C. H. *Phys. Rev.* **1941**, *60*, 252.

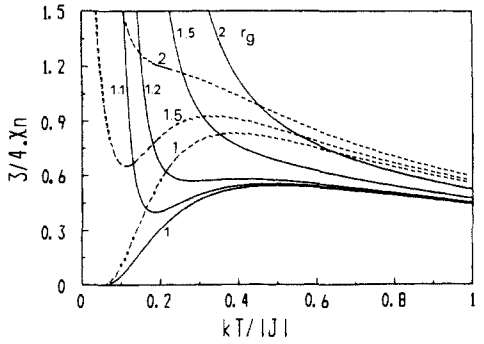

Figure 8. Theoretical variation of the normalized magnetic susceptibility $\chi_n = \chi|J|/(Ng^2\mu_B^2)$ showing the influence of the relative g factors ($r_g = g_a/g_b$) in the limiting cases $j = J$ (full lines) and $j = 0$ (dashed lined).

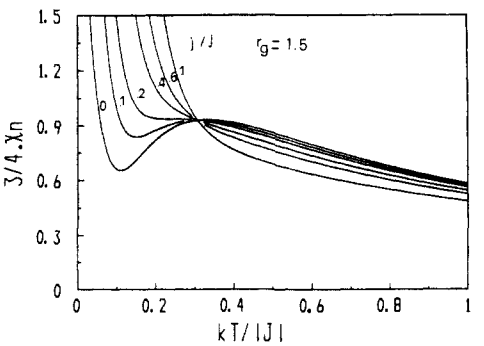

Figure 9. Theoretical variation of the normalized magnetic susceptibility for some significant values of the ratio between the exchange constants j and J and $g_a/g_b = 1.5$.

For a nonvanishing magnetic field, the partition function is given by

$$Z(H) = ab\cosh(g_+u_BH/kT) + a^{-1}b^{-1}\cosh(g_-u_BH/kT) + ((ab\cosh(g_+u_BH/kT) + a^{-1}b^{-1}\cosh(g_-u_BH/kT))^2 - 4\sinh(J/2kT)\sinh(j/2kT))^{1/2} \quad (2)$$

$$\text{with} \quad g_\pm = (g_a \pm g_b)/2$$

In the $H \to 0$ limit, this expression reduces to

$$Z = 2(\cosh(J_+/2kT) + \cosh(J_-/2kT)) \quad (3)$$

$$\text{where } J_\pm = (J \pm j)/2$$

Then, it is straightforward to deduce the zero-field specific heat

$$C/R = (1/4kT)^2(J^2\,\mathrm{sech}^2(J/4kT) + j^2\,\mathrm{sech}^2(j/4kT)) \quad (4)$$

Of course, this expression agrees fully with the well-known formulas derived for the dimer ($j = 0$) and the chain ($J = j$) limits. In the intermediate case ($j = J$), the specific heat is merely described as the sum of two Schottky-type contributions. Clearly, the position on the temperature axis of the respective maxima and the spread of the bumps are both related to the values of the exchange parameters j and J. In this respect, we should observe an asymmetrical Schottky anomaly for j of the order of J (with $j \neq J$).

Returning to the general expression of the partition function, we readily calculate the magnetization from the first derivative of $\ln(Z)$ with respect to H

$$M(H) = u_B(g_+ab\sinh(g_+u_BH/kT) + g_-a^{-1}b^{-1}\sinh(g_-u_BH/kT) + (g_+a^2b^2\sinh(g_+u_BH/kT)\cosh(g_+u_BH/kT) + g_-a^{-2}b^{-2}\sinh(g_-u_BH/kT)\cosh(g_-u_BH/kT) + \tfrac{1}{2}g_a\sinh(g_au_BH/kT) + \tfrac{1}{2}g_b\sinh(g_bu_BH/kT))/(Z(H) - ab\cosh(g_+u_BH/kT) - a^{-1}b^{-1}\cosh(g_-u_BH/kT))) \quad (5)$$

We further deduce the zero-field parallel susceptibility given by

$$\chi_\parallel = (Nu_B^2/2kT) \times (g_+^2\exp(J_+/2kT) + g_-^2\exp(-J_+/2kT))/\cosh(J_-/2kT) \quad (6)$$

Note that this expression refers to a two-spin subunit. For $a = b$ and $j = J$, it reduces to the susceptibility of the regular Ising chain as derived by Fisher.[17]

The influence of the g alternation is reported in Figure 8 for two limiting cases, namely the regular chain ($j = J$) and the dimer unit ($j = 0$). The results correspond to the normalized susceptibility, $\chi_n = \chi_\parallel|J|/(Ng_\parallel^2\mu_B^2)$; putting $g_\parallel^2 = (g_{a\parallel}^2 + g_{b\parallel}^2)/2$ allows us to obtain a uniform behavior in the high-temperature limit. For the J regular chain, the maximum of χ is conserved as long as the ratio between the Landé factors (r_g) is close to unity. For increasing r_g, a rapid divergence of $\chi_\parallel$ (and even of the $\chi_\parallel T$ product), due to the nonzero magnetic moment in the ground state, occurs upon cooling down, thus masking this maximum. Conversely, in the dimer limit the curves of $\chi_\parallel$ versus T (and also of $\chi_\parallel T$) exhibit a less drastic variation at low temperature. The maximum is observed over a larger range of r_g values; on the other hand, the product $\chi_\parallel T$ is expected to show a constant value, as $T \to 0$, in agreement with the noncompensated magnetic moment of the pair.

In intermediate cases where both j/J and $r_g = g_a/g_b$ differ from unity, one finds that, for $r_g \gg 1$, the maximum of susceptibility is only noticeable near the dimer limit. As an example, the magnetic behavior is displayed, in Figure 9, for $r_g = 1.5$ and some significant values of j/J.

Notice that the above discussion concerns the parallel component to the susceptibility. This direction refers to the external magnetic field with respect to the spin-quantization axis without preconception about the direction of the chains.

Clearly, the expression of the perpendicular susceptibility cannot be determined in the same way. By using the technique developed by Fisher[17] (the susceptibility is expressed in terms of high-order spin correlation functions) we have derived an exact closed formula in the limiting case of the g alternating chain with a single exchange constant. The result is of the same kind as Fisher's expression for the compensated antiferromagnetic chain, namely

$$\chi_\perp = (Ng_\perp^2u_B^2/2J)(\tanh(J/4kT) + (J/4kT)\,\mathrm{sech}^2(J/4kT)) \quad (7)$$

where now

$$g_\perp^2 = (g_{a\perp}^2 + g_{b\perp}^2)/2$$

In the other limit (Ising dimer), the susceptibility reduces to

$$\chi_\perp = (2Ng_\perp^2\mu_B^2/J)\tanh(J/4kT) \quad (8)$$

Notice that the perpendicular susceptibility does not give any information about the nature of a chain (ferri- or antiferromagnetic). The product $\chi_\perp T$ decreases toward zero upon cooling down; as a result, the divergence of χT observed experimentally when studying powders of 1d ferrimagnets should be due to the parallel component of the susceptibility. We will assume in the following that this result also holds for the J alternating ferrimagnetic chain.

Analysis and Discussion

Before discussing the magnetic data of the systems under consideration, it is worthwhile to note that, due the structural features of the zigzag chains, the g tensors for both sites have different orientations with respect to the principal magnetic axes. Accordingly, the g parameters deduced from the magnetic data can differ significantly from those obtained by EPR measurements. However, the EPR findings are still useful in the analysis of the susceptibility results, since they restrict the range of available r_g values in the fitting procedure. So, assuming that the main axes are fixed by the most anisotropic ion and taking further into account the limiting g values for both ions, one may anticipate that r_g ranges between 0.4 and 4.8 in [CoCo] and between 1.7 and 2.9 in [CoCu].

Magnetic Susceptibility Results. We have shown previously that a simple antiferromagnetic Heisenberg model is inadequate

(17) Fischer, M. E. *J. Math. Phys.* **1963**, *4*, 124.

Table I. Best Fit Parameters of [CoCo] and [CoCu] from Magnetic Susceptibility and Specific Heat Studies

	$\chi_M = f(T)$					$C/R = f(T)$			
						$(J-j)$ Ising chain		anisotropic dimer	
	$g_{a\parallel}$	$g_{b\parallel}$	$g_\perp$	J (K)	j (K)	J (K)	j (K)	J (K)	$J_\perp/J_\parallel$
[CoCo]	3.99	1.33	3.03	−10.2	−0.12	−18.6	−7.1	−17.5	0.22
	5.33	2.48	3.75	−17.5	−0.05				
[CoCu]	4.31	2.63	0	−3.2	−0.05	−4.4	−3.7	−4.5	0.35

for describing the low-temperature magnetic properties of the [CoCo] and [CoCu] compounds. More insight into their behavior requires, in fact, the use of an anisotropic exchange model, with both alternating Landé factors and alternating exchange interactions.

Notwithstanding, it is to recall that whereas the parallel component to the susceptibility has been solved for the J alternating chain, the perpendicular component is only available in the two limiting cases pointed out above. Then, the fit of the data from the expression of the average susceptibility, $\chi = {}^1/_3(\chi_\parallel + 2\chi_\perp)$, necessitates to choose between the two limiting solutions for χ. In any case, the fact that the perpendicular contribution is weak and only slightly temperature dependent in the region of interest makes this choice of minor relevance. Further, the specific features of the two sublattice Ising system are mainly accounted for by the parallel component of χ.

On closer examination of eq 6, it appears in fact that for large J_- values and $kT \ll |J_-|$, χ reduces to

$$\chi = (N\mu_B^2/kT)(g_+^2 \exp(J/2kT) + g_-^2 \exp(-j/2kT)) \quad (9)$$

Then, the low-temperature divergence of χ is clearly related only to the parameters j and g_-. In this respect, the fitting procedure is straightforward since an estimate of these parameters can be obtained by plotting the low-temperature data as $\log(\chi T)$ versus $1/T$. Thus, for both systems the j parameter was shown to be very small but different from zero as evidenced by the divergence of χT below 0.2 K.

In view of these results, the magnetic data of [CoCo] and [CoCu] were fitted, in the range 0.1–4 K, by assuming as the perpendicular component to the susceptibility that of the dimer system. The best fitted curves obtained by least-squares refinement are illustrated in Figures 3 and 4. The resulting parameters are listed in Table I.

For [CoCo], several sets of parameters giving close agreement with the experiment were found with J ranging between −10 and −18 K and j close to zero. In all cases, the continuous variation of the susceptibility with temperature and its drastic increase as $T \to 0$ are well reproduced by theory. This result is somewhat surprising if we look at the values obtained for the (g_a, g_b) sets, the mean values of which are in a ratio of about 2. In fact, we have shown above that g_- is the only relevant parameter to explain the divergence of the susceptibility. Accordingly, it stays relatively constant in the reported fits. In turn, the mean value g_+, which acts at higher temperatures, is not determined unambigously ($\chi_\perp$ and the first term of eq 9 are no longer negligible when T increases), so that we must be cautious to draw conclusions about the g_a and g_b parameters.

The above remarks hold equally well for [CoCu]. As can be seen from Figure 4, we obtain a very good description of the magnetic susceptibility over the entire temperature region of interest. In particular, the rounded maximum, not observed for the pure cobalt chain, and the fast increase upon cooling down are well reproduced by the model. The Landé factors resulting from the analysis, $g_a = 4.31$ and $g_b = 2.63$, agree reasonably well with the values expected for cobalt(II) and copper(II) ions in similar environments. Moreover, note that g_-, responsible for the low-temperature divergence of χ is very close to the value obtained for [CoCo].

The "quasi" antiferromagnetic behavior shown by this compound can be described equally from other sets of parameters involving r_g values close to unity; for instance $J = -4.5$ K, $j = -1.2$ K, $g_{a\parallel} = 5.00$, $g_{b\parallel} = 5.40$, and $g_\perp = 2.73$. These results have been ruled out since the corresponding r_g ratios fall much below the range of available values ($r_{gmin} = 1.7$).

Specific Heat Results. The magnetic contribution to the specific heat of both [CoCo] and [CoCu] complexes are displayed in Figures 6 and 7. It should be noted that not all of the data have been used. The high-temperature region ($T > 10$ K) has been excluded, because of the decreasing accuracy mentioned before.

As predicted, both specific heat curves show a Schottky-type anomaly, but on closer examination significant differences are seen, as for instance in the shape and the position in temperature of the maximum. By fitting the data to the available expression for C/R (eq 4) we obtain the values of the exchange parameters listed in Table I.

Note, at first, the very good agreement with theory of the specific heat for both systems (full lines). On the basis of the J alternating Ising model, the broad and asymmetric bump observed in [CoCo] may be well-described by an alternation of the exchange coupling ($j/J = 0.38$). Contrastingly, the narrow and symmetric bump observed for [CoCu] agrees with a weakly alternating exchange coupling ($j/J = 0.84$). Nevertheless, these results differ widely from those of the magnetic susceptibility which pointed to a very significant dimerization. Actually, we must recall that the above analysis is based on the Ising model, which seems justified for describing the highly anisotropic cobalt(II) ion (as the "chelated" cobalt in [CoCo]) but becomes questionable for describing the [CoCu] system, and then it may be stated that the interactions are possibly in between the Ising and Heisenberg limits.

Since the susceptibility indicated a strong degree of dimerization, we have also fitted the specific heat data to predictions from the anisotropic dimer model, the solution of which is easily derived. It is clear that an anisotropic chain model with alternating exchange would be more suitable, but the solutions are not available. The best fitted curves are plotted in Figures 6 and 7 (dashed lines), and the resulting parameters are reported in Table I. It appears that this model gives a good description of the specific heat data for both systems. Further, according to the expected trend, the amount of anisotropy is significantly less in [CoCu] than in [CoCo]. In view of these results, the specific heat curves appear to be very sensitive to the anisotropy of the exchange coupling, to a similar order as to the alternating interaction.

Finally, these results are now consistent with those of the magnetic susceptibility pointing to a strong dimerization. Thus, the exchange parameters obtained by the specific heat analysis allow to obtain a satisfactory fit of the magnetic data in both cases. We note that although a significant alternation of the J value is found for both systems, this does not alter basically the ferrimagnetic character of the chains.

Conclusion

We have discussed in this paper the thermal and magnetic properties of two spin-1/2 alternating chain systems, namely $Co_2(EDTA)\cdot 6H_2O$ and $CoCu(EDTA)\cdot 6H_2O$, exhibiting the typical features of 1d-ferrimagnets. So far, the 1d-ferrimagnetism was reported in bimetallic complexes characterized by noncompensated spin sublattices. In the above examples, we show that different g values at different (alternating) sites give rise to the same characteristic behavior, even for a large dimerization of the chains. In fact the mechanism is more subtle; the ferrimagnetic behavior may also result from the presence of anisotropic g tensors at two consecutive sites, exhibiting different orientations with

Table II. Final Characterization of [CoCo] and [CoCu]

		g_1	g_2	g_3	J^a (K)	$\|j\|^a$ (K)	$\alpha = J_\perp/J_\parallel$
	$(Co)_h^b$	5.90	3.88		-6.3	<0.05	0.22
[CoCo]	$(Co)_q$	10.1	1.43	1.24			
[CoCu]	$(Cu)_q$	2.27	2.02		-2.7	<0.05	0.35

[a] Scaling factors have been introduced to account for the effective spin of Co(II) (these factors are 9/25 for [CoCo] and 3/5 for [CoCu]. [b] h and q refer to the "hydrated" and "chelated" sites, respectively.

respect to the principal magnetic axes.

Considering both the alternation of the Landé factors and the alternating character of the exchange coupling, we have derived the exact solutions for the spin-1/2 Ising chain and compared the results to the experiment. Although the analysis of the above systems is not straightforward, a reasonable agreement between the parameters determined from different (and complementary) experiments was obtained. Thus, the magnetic susceptibility data appeared to be very useful to emphasize the strong dimerization of the chains ($j/J < 0.05$). Conversely, due to the large number of adjustable parameters used in the magnetic analysis, it results in a large uncertainty in their absolute values.

In turn, the specific heat results have shown to be relatively insensitive to the dimensionality of these systems. Thus, the Schottky anomaly can be well-explained in terms of (alternating) Ising chains or by assuming anisotropic exchange coupled dimers. In view of the magnetic susceptibility analysis, the second model seems to be the more realistic. Finally, due to the limited number of parameters in the specific heat analysis, we obtain reliable values for J and α.

Hence, from the above results and the EPR findings, we have a satisfying characterization of both compounds (Table II).

The strong difference between J and j observed in both cases cannot be explained by simple structural arguments (metal–metal distances or bond angles of bridging ligands, for instance). In turn, by focusing on the zigzag chain structure, and the directions of anisotropy for the Ising-type ions, it is likely that quantum effects do induce a significant alternation in the exchange coupling. In this respect, a rigorous analysis of the exchange mechanisms accounting for the above effects and the available overlap between metallic magnetic orbitals (via bridging atoms) is not straightforward in the present case.

Finally, in regards to the interchain interactions, it is worth noticing that their influence is negligible in both systems (no λ-type anomaly in the specific heat data), while they are quite prominent in the related systems [MnCo], [MnNi], and [MnCu]. The manifestation of such interactions is obviously closely related to the ground spin configuration of the chain. Thus, drastic effects are anticipated for 1d ferrimagnets with two distinct spins (high spin ground state), but, conversely, the effect will be of the second order when only g factors alternate (the ground configuration is $S = 0$). This warrants the description of [CoCo] and [CoCu] in terms of well-isolated dimerized chains.

Acknowledgment. This work was supported in part by the European Economic Community (Grant ST2/164) and the Comision Asesora de Investigaciones Cientificas y Tecnicas (2930/83). One of us (E.C.) has also obtained a grant from Generalitat Valenciana.

Registry No. [CoCo], 84222-22-0; [CoCu], 84222-24-2.

Metal-Assisted Three-Fragment Demolition of the Dithiocarbonate Ligand: A New Synthetic Route to Homo- and Heterobinuclear Bis(μ-sulfido)metal Complexes. Chemical, Electrochemical, and Spectroscopic Characterization of a Family of Complexes of Iron, Cobalt, Rhodium, and Platinum with Bridging Sulfido Ligands

Claudio Bianchini,*† Andrea Meli,† Franco Laschi,‡ Alberto Vacca,† and Piero Zanello‡

Contribution from the Istituto per lo Studio della Stereochimica ed Energetica dei Composti di Coordinazione, CNR, Via J. Nardi 39, 50132 Firenze, and Dipartimento di Chimica, Università di Siena, Pian dei Mantellini, Siena, Italy. *Received September 22, 1987*

Abstract: Homo- and heterobinuclear bis(μ-sulfido) complexes of the general formula $[(triphos)Rh(\mu\text{-}S)_2M(L)](BPh_4)_x$ [M = Rh, L = triphos, $x = 2$; M = Co, L = triphos, $x = 1, 2$; M = Pt, L = diphos, $x = 1$; M = Fe, L = etriphos and CO, $x = 1$] [triphos = $MeC(CH_2PPh_2)_3$; diphos = $Ph_2PCH_2CH_2PPh_2$; etriphos = $MeC(CH_2PEt_3)_2$] are obtained by reaction of the dithiocarbonates $[(triphos)Rh(S_2CO)]BPh_4$ or $(triphos)Co(S_2CO)$ with coordinatively unsaturated fragments. The reactions proceed through chelotropic elimination of carbon monoxide from the RhSCOS or CoSCOS cycles promoted by interaction of the externally added metal fragment with the two sulfur atoms of the dithiocarbonate ligands. The electrochemical behavior in CH_2Cl_2 solution of all of the bis(μ-sulfido) dimers has been investigated. In particular, the complexes containing the $Rh(\mu\text{-}S)_2Rh$, $Rh(\mu\text{-}S)_2Co$, and $Co(\mu\text{-}S)_2Co$ cores undergo electron-transfer reactions that encompass the 0, 1+, and 2+ charges with no change of the primary geometry. By contrast, the compounds with the $Rh(\mu\text{-}S)_2Fe$ and $Rh(\mu\text{-}S)_2Pt$ cores rapidly decompose on addition of electrons. Chemical and electrochemical techniques have been used to prepare the paramagnetic congeners $[(triphos)Rh(\mu\text{-}S)_2Rh(triphos)]BPh_4$ and $[(triphos)Rh(\mu\text{-}S)_2Co(triphos)]BPh_4$. The products have been characterized by IR, ^{31}P NMR, and ESR spectroscopies. The reactions of the compounds with molecular hydrogen have been investigated.

Binuclear complexes with sulfido bridges are of current interest, owing to their use as models for biological systems,[1] as well as the variety of their application in stoichiometric[2] and catalytic reactions.[2i] Also, a great number of sulfido-bridged dimers display extensive electron-transfer chemistry, which does not destroy the

† CNR.
‡ Università di Siena.

(1) Berg, J. M.; Holm, R. H. In *Metal Ions in Biology*; Spiro, T. G., Ed.; Wiley-Interscience: New York, 1982; Vol. 4, Chapter 1.

0002-7863/88/1510-3913$01.50/0